

Mononuclear and Dendritic Nickel(II) Complexes Containing N,N' -Iminopyridine Chelating Ligands: Generation Effects on the Catalytic Oligomerization and Polymerization of Ethylene[†]

José M. Benito, Ernesto de Jesús,* F. Javier de la Mata, Juan C. Flores,*
Rafael Gómez, and Pilar Gómez-Sal

Departamento de Química Inorgánica, Universidad de Alcalá, Campus Universitario,
28871 Alcalá de Henares, Madrid, Spain

Received October 19, 2005

A series of carbosilane dendritic compounds G_n -ONNMe_{*m*}, containing one ($n = 0$), four ($n = 1$), eight ($n = 2$), or 16 ($n = 3$) terminal pyridylimine ligands, substituted with m methyl groups ($m = 0, 2, 3$), and nickel complexes G_n -ONNMe_{*m*}NiBr₂, comprising monometallic to metallodendritic structures, have been synthesized. The nickel complexes, in combination with methylaluminoxane (MAO), are active catalysts for the concurrent transformation of ethylene into mixtures of toluene-insoluble polyethylene and oily oligomers. Oligomers consist of mixtures of olefins that follow a Schulz–Flory distribution, and polymers are found to be highly branched low molecular weight polyethylene. The variation of the pyridylimine ligand framework by methyl substituents has a decisive influence on the activities of the nickel compounds. Also, the size (i.e., generation n) of the dendritic precursor acutely affects the catalyst performance and the microstructure of the insertion products. Thus, higher generation catalysts show superior oligomerization activities and produce less branched polyethylene polymers with higher molecular weights.

Introduction

The interest in the field of well-defined late transition metal catalysts for olefin polymerization has been renewed during the last decade.¹ Following the disclosures by Brookhart² and by Gibson,³ most of these catalysts have been based on nickel and palladium α -diimine-based complexes, or iron or cobalt compounds bearing bis(imino)pyridyl ligands. Earlier work by Keim showed that Ni(II) complexes containing bidentate P/O chelating ligands are effective homogeneous catalysts for the oligomerization of ethylene (SHOP process),⁴ affording α -olefins in the industrially desirable C₄–C₂₀ range.⁵ The oligomers are produced due to a highly competitive chain transfer reaction relative to chain propagation.⁶ The chain termination rate is retarded by using Brookhart-type Ni(II) catalysts with sterically demanding α -diimine ligands, which block the axial sites of the active center, impeding the chain transfer process and thus enhancing its growth.^{2,6} Consequently, depending on the substitution of the ligand and the reaction conditions, these catalysts produce

ethylene derivatives ranging from light oligomers to high molecular weight polymers,^{2,7–11} with linear to hyperbranched microstructures as a result of the so-called “chain-walking mechanism”.¹² Considerable effort has been made to expand the scope of chelating ligands on nickel and palladium complexes useful in ethylene chemistry,¹ including studies with P/O,¹³ N/O,¹⁴ P/P,¹⁵ and N/P¹⁶ bidentate systems. Asymmetrical N/N pyridylimine-type compounds have also been synthesized and used as catalysts in ethylene oligomerization and polymerization reactions.^{17–21} In addition, this class of ligands has been successfully applied in solid-phase organometallic synthesis

(7) Deng, L.; Woo, T. K.; Cavallo, L.; Margl, P. M.; Ziegler, T. *J. Am. Chem. Soc.* **1997**, *119*, 66177.

(8) (a) Killiam, C. M.; Johnson, L. K.; Brookhart, M. *Organometallics* **1997**, *16*, 2005. (b) Svejda, S. A.; Brookhart, M. *Organometallics* **1999**, *18*, 65.

(9) (a) Helldörfer, M.; Backhaus, J.; Milius, W.; Alt, H. G. *J. Mol. Catal. A: Chem.* **2003**, *193*, 59. (b) Helldörfer, M.; Milius, W.; Alt, H. G. *J. Mol. Catal. A: Chem.* **2003**, *197*, 1. (c) Helldörfer, M.; Backhaus, J.; Alt, H. G. *Inorg. Chim. Acta* **2003**, *351*, 34.

(10) Maldanis, R. J.; Wood, J. S.; Chandrasekaran, A.; Rausch, M. D.; Chien, J. C. W. *J. Organomet. Chem.* **2002**, *645*, 158.

(11) Schleis, T.; Spaniol, T. P.; Okuda, J.; Heinemann, J.; Mühlaupt, R. *J. Organomet. Chem.* **1998**, *569*, 159.

(12) (a) Svejda, S. A.; Johnson, L. K.; Brookhart, M. *J. Am. Chem. Soc.* **1999**, *121*, 10634. (b) Tempel, D. J.; Johnson, L. K.; Huff, R. L.; White, P. S.; Brookhart, M. *J. Am. Chem. Soc.* **2000**, *122*, 6686. (c) Leatherman, M. D.; Svejda, S. A.; Johnson, L. K.; Brookhart, M. *J. Am. Chem. Soc.* **2003**, *125*, 3068.

(13) (a) Mecking, S.; Keim, W. *Organometallics* **1996**, *15*, 2650. (b) Komon, Z. J. A.; Bu, X.; Bazan, G. C. *J. Am. Chem. Soc.* **2000**, *122*, 12379. (c) Liu, W.; Malinoski, J. M.; Brookhart, M. *Organometallics* **2002**, *21*, 2836. (d) Heinicke, J.; Koesling, M.; Brüll, R.; Keim, W.; Pritzkow, H. *Eur. J. Inorg. Chem.* **2000**, 299.

(14) (a) Wang, C.; Friedrich, S.; Younkin, T. R.; Li, R. T.; Grubbs, R. H.; Bansleben, D. A.; Day, M. W. *Organometallics* **1998**, *17*, 3149. (b) Younkin, T. R.; Connor, E. F.; Henderson, J. I.; Friedrich, S. K.; Grubbs, R. H.; Bansleben, D. A. *Science* **2000**, *287*, 460. (c) Hicks, F. A.; Brookhart, M. *Organometallics* **2001**, *20*, 3217. (d) Speiser, F.; Braunstein, P. *Inorg. Chem.* **2004**, *43*, 4234.

[†] Dedicated to Prof. Dr. Victor Riera on the occasion of his 70th birthday.

* Corresponding authors. Tel: +34 91 885 4603 (E.J.); +34 91 885 4607 (J.C.F.). Fax: +34 91 885 4683. E-mail: ernesto.dejesus@uah.es (E.J.); juanc.flores@uah.es (J.C.F.).

(1) For recent reviews see: (a) Gibson, V. C.; Spitzmesser, S. K. *Chem. Rev.* **2003**, *103*, 283. (b) Ittle, S. D.; Johnson, L. K.; Brookhart, M. *Chem. Rev.* **2000**, *100*, 1169. (c) Mecking, S. *Coord. Chem. Rev.* **2000**, *203*, 325.

(2) Johnson, L. K.; Killian, C. M.; Brookhart, M. *J. Am. Chem. Soc.* **1995**, *117*, 6414.

(3) Britovsek, G. J. P.; Gibson, V. C.; Kimberley, B. S.; Maddox, P. J.; McTavish, S. J.; Solan, G. A.; White, A. J. P.; Williams, D. J. *Chem. Commun.* **1998**, 849.

(4) (a) Keim, W.; Kowalt, F. H.; Goddard, R.; Krüger, C. *Angew. Chem., Int. Ed. Engl.* **1978**, *17*, 466. (b) Peuckert, M.; Keim, W. *Organometallics* **1983**, *2*, 594. (c) Keim, W. *Angew. Chem., Int. Ed. Engl.* **1990**, *29*, 235.

(5) Vogt, D. *Applied Homogeneous Catalysis with Organometallic Compounds*; Cornils, B., Hermann, W. A., Eds.; VCH: Weinheim, 1996; Vol. 1, p 245.

(6) Skupinska, J. *Chem. Rev.* **1991**, *91*, 613.

and radical polymerization, by immobilizing molybdenum carbonyl²² and copper halide complexes,²³ respectively.

Research on metallodendrimers has also been a prominent area during the last few years, and an increasing number of reports have been published on the incorporation of transition metals at the core, branches, or periphery of dendrimers.²⁴ Encouraged by the fact that dendrimers can be used as well-defined supports for active centers in a homogeneous phase, their catalytic applications are being widely studied,²⁵ including those in polymerization,^{18b,26–29} and oligomerization processes.³⁰

We have recently initiated a program focused on the chemistry of carbosilane dendrimers containing early transition metal complexes located at the dendritic periphery, or at the focal point,³¹ and usually bonded through O-³² or N-donor³³

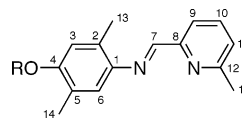


Figure 1. Numbering scheme for pyridylimine fragment.

anchoring ligands. As part of this research and in an attempt to expand the range of useful synthetic routes available to attach metal complexes to dendrimers, we decided to evaluate the possible application of pyridylimine ligands (Figure 1) in the field of carbosilane metallodendritic chemistry and analyze relationships between the dendritic nature of nickel derivatives and their polymerization behavior. Since dendritic moieties bring about distinctive catalytic environments, and ethylene polymerization with late transition metal catalysts is sensitive to the active site surroundings, we decided to extend and explore the capacity of metallodendrimer chemistry in this type of process. This paper describes the synthesis and characterization of different pyridylimine-ended carbosilane dendrimers and their subsequent complexation with nickel(II), as well as monometallic nickel model complexes. In addition, the results using the nickel compounds as catalyst precursors for ethylene polymerization are also presented. The influence of the dendrimer generation and the substitution of the N/N anchoring ligand on the catalytic potential are analyzed. A preliminary account of part of this work has been published previously.^{33d}

Results and Discussion

Synthesis of Ligands and Mononuclear Nickel Compounds. The pyridylimine ligands used in this work are the N-donor bidentates **1a–c** (Scheme 1), with an unprotected phenolic hydroxy group effective for the functionalization of dendrimers, and the trimethylsilyl-protected derivatives **2a–c**, useful as models of the dendritic carbosilanes described further on. They were synthesized adapting a procedure described in the literature for **1a** and **2a**, which consists of the condensation of pyridine-2-carbaldehyde or 6-methylpyridine-2-carbaldehyde with the corresponding *p*-aminophenol compound, accompanied in the case of **2** by the phenolysis of chlorotrimethylsilane.^{22a} The sequence of reactions can be inverted as demonstrated in the preparation of **2a** (see Experimental Section and Scheme 1). Compounds **1** and **2** were isolated in high yields as yellow solids and oils, respectively. All compounds gave satisfactory elemental analyses, and their mass spectra (EI/MS) exhibit a peak assignable to the molecular ion. The relevant feature of their ¹H and ¹³C NMR spectra is the appearance of two singlets for the Me¹³ and Me¹⁴ groups (numbering in Figure 1; $\delta =$

(15) (a) Ikeda, S.; Ohhata, F.; Miyoshi, M.; Tanaka, R.; Minami, T.; Ozawa, F.; Yoshifuji, M. *Angew. Chem., Int. Ed.* **2000**, *39*, 4512. (b) Cooley, N. A.; Green, S. M.; Wass, D. F.; Heslop, K.; Orpen, A. G.; Pringle, P. G. *Organometallics* **2001**, *20*, 4769. (c) Albers, I.; Alvarez, E.; Cámpora, J.; Maya, C. M.; Palma, P.; Sánchez, L. J.; Passaglia, E. *J. Organomet. Chem.* **2004**, *689*, 833.

(16) (a) Guan, Z.; Marshall, W. J. *Organometallics* **2002**, *21*, 3580. (b) Daugulis, O.; Brookhart, M. *Organometallics* **2002**, *21*, 5926. (c) Daugulis, O.; Brookhart, M.; White, P. S. *Organometallics* **2002**, *21*, 5935.

(17) (a) Laine, T. V.; Lappalainen, K.; Liimatta, J.; Aitola, E.; Löfgren, B.; Leskelä, M. *Macromol. Rapid Commun.* **1999**, *20*, 487. (b) Laine, T. V.; Klinga, M.; Leskelä, M. *Eur. J. Inorg. Chem.* **1999**, 959. (c) Laine, T. V.; Piironen, U.; Lappalainen, K.; Klinga, M.; Aitola, E.; Leskelä, M. *J. Organomet. Chem.* **2000**, *606*, 112.

(18) (a) Chen, R.; Bacsa, J.; Mapolie, S. F. *Inorg. Chem. Commun.* **2002**, *5*, 724. (b) Smith, G.; Chen, R.; Mapolie, S. J. *Organomet. Chem.* **2003**, *673*, 111. (c) Chen, R.; Mapolie, S. F. *J. Mol. Catal. A: Chem.* **2003**, *193*, 33.

(19) (a) Köppl, A.; Alt, H. G. *J. Mol. Catal. A: Chem.* **2000**, *154*, 45. (b) Köppl, A.; Alt, H. G. U.S. Patent 5932670 (Phillips Petroleum Company, USA), 1999.

(20) Eilerts, N. W. PCT Int. Appl. WO 99/49969 (Phillips Petroleum Company, USA), 1999.

(21) Bres, P.-L.; Gibson, V. C.; Mabile, C. D.; Reed, W.; Wass, D.; Weatherhead, R. H. PCT Int. Appl. WO 98/49208 (BP Chemicals, GB), 1998.

(22) (a) Heinze, K. *Chem. Eur. J.* **2001**, *7*, 2922. (b) Heinze, K.; Jacob, V.; Feige, C. *Eur. J. Inorg. Chem.* **2004**, 2053.

(23) Haddleton, D. M.; Kukulj, D.; Radigue, A. P. *Chem. Commun.* **1999**, 99.

(24) (a) Gorman, C. *Adv. Mater.* **1998**, *10*, 295. (b) Newkome, G. R.; He, E.; Moorefield, C. N. *Chem. Rev.* **1999**, *99*, 1689. (c) Cuadrado, I.; Morán, M.; Casado, C. M.; Alonso, B.; Losada, J. *Coord. Chem. Rev.* **1999**, *193–195*, 395. (d) Stoddart, F. J.; Welton, T. *Polyhedron* **1999**, *18*, 3575. (e) Hearshaw, M. A.; Moss, J. R. *Chem. Commun.* **1999**, 1. (f) van Manen, H.-J.; van Veggel, F. C. J. M.; Reinhoudt, D. N. *Top. Curr. Chem.* **2001**, *217*, 121. (g) Onitsuka, K.; Takahashi, S. *Top. Curr. Chem.* **2003**, *228*, 39. (h) Chase, P. A.; Gebbink, R. J. M. K.; van Koten, G. *J. Organomet. Chem.* **2004**, *689*, 4016. (i) Rossell, O.; Seco, M.; Angurell, I. C. R. *Chim.* **2003**, *6*, 803.

(25) (a) Oosterom, G. E.; Reek, J. N. H.; Kamer, P. C. J.; van Leeuwen, P. W. N. M. *Angew. Chem., Int. Ed.* **2001**, *40*, 1828. (b) Astruc, D.; Chardac, F. *Chem. Rev.* **2001**, *101*, 2991. (c) van Heerbeek, R.; Kamer, P. C. J.; van Leeuwen, P. W. N. M.; Reek, J. N. H. *Chem. Rev.* **2002**, *102*, 3717. (d) Kreiter, R.; Kleij, A. W.; Gebbink, R. J. M. K.; van Koten, G. *Top. Curr. Chem.* **2001**, *217*, 163. (e) Caminade, A. M.; Maraval, V.; Laurent, R.; Majoral, J. P. *Curr. Org. Chem.* **2002**, *6*, 739. (f) Dahan, A.; Portnoy, M. *J. Polym. Sci. A Polym. Chem.* **2005**, *43*, 235. (g) van de Coevering, R.; Klein Gebbink, R. J. M.; van Koten, G. *Prog. Polym. Sci.* **2005**, *30*, 474. (h) Méry, D.; Astruc, D. *Coord. Chem. Rev.* **2006**, in press, doi: 10.1016/j.ccr.2005.11.012.

(26) Seyferth, D.; Wrywra, R.; Franz, U. W.; Becke, S. PCT Int. Appl. WO 97/32908 (BAYER), 1997.

(27) Zheng, Z.-J.; Chen, J.; Li, Y.-S. *J. Organomet. Chem.* **2004**, *689*, 3040.

(28) Matyjaszewski, K.; Shigemoto, T.; Fréchet, J. M. J.; Leduc, M. *Macromolecules* **1996**, *29*, 4167.

(29) (a) Gatard, S.; Kahlal, S.; Méry, D.; Nlate, S.; Cloutet, E.; Saillard, J.-Y.; Astruc, D. *Organometallics* **2004**, *23*, 1313. (b) Gatard, S.; Nlate, S.; Cloutet, E.; Bravic, G.; Blais, J.-C.; Astruc, D. *Angew. Chem., Int. Ed.* **2003**, *42*, 452.

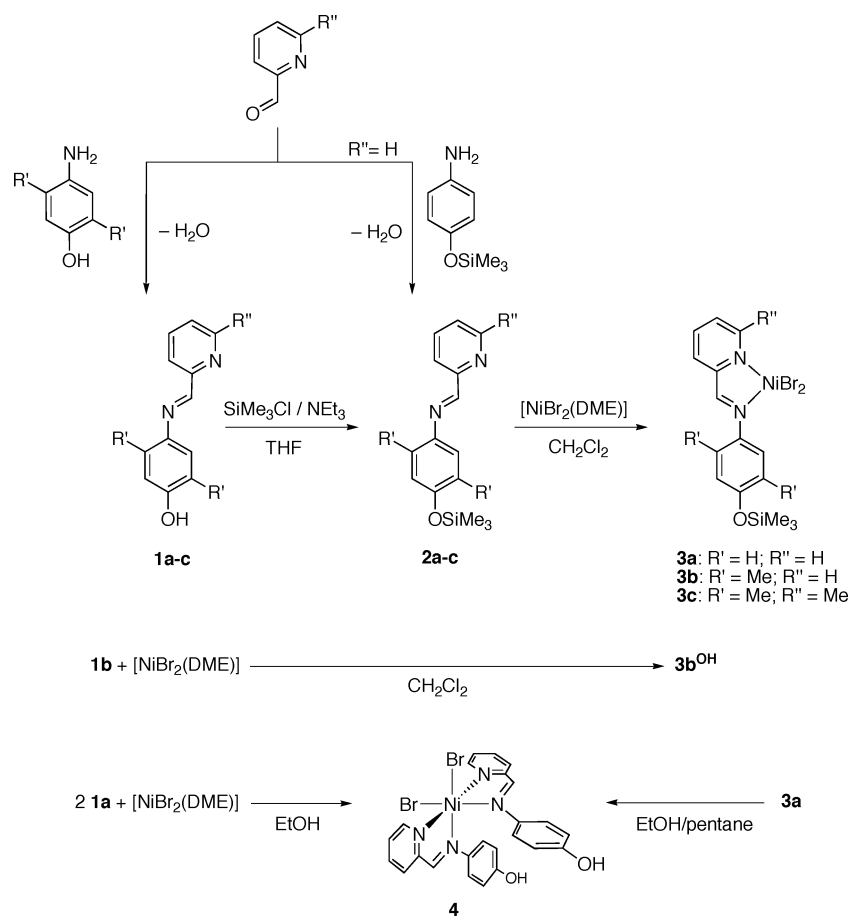
(30) (a) Müller, C.; Ackerman, L. J.; Reek, J. N. H.; Kamer, P. C. J.; van Leeuwen, P. W. N. M. *J. Am. Chem. Soc.* **2004**, *126*, 14960. (b) Overett, M. J.; Meijboom, R.; Moss, J. R. *Dalton Trans.* **2005**, 551.

(31) (a) Andrés, R.; de Jesús, E.; de la Mata, F. J.; Flores, J. C.; Gómez, R. *Eur. J. Inorg. Chem.* **2002**, 2281. (b) Andrés, R.; de Jesús, E.; de la Mata, F. J.; Flores, J. C.; Gómez, R. *J. Organomet. Chem.* **2005**, *690*, 939. (c) Amo, V.; Andrés, R.; de Jesús, E.; de la Mata, F. J.; Flores, J. C.; Gómez, R.; Gómez-Sal, P.; Turner, J. F. C. *Organometallics* **2005**, *24*, 2331. (d) Andrés, R.; de Jesús, E.; de la Mata, F. J.; Flores, J. C.; Gómez, R. *Eur. J. Inorg. Chem.* **2005**, 3742.

(32) (a) Arévalo, S.; Benito, J. M.; de Jesús, E.; de la Mata, F. J.; Flores, J. C.; Gómez, R. *J. Organomet. Chem.* **2000**, *602*, 208. (b) Arévalo, S.; de Jesús, E.; de la Mata, F. J.; Flores, J. C.; Gómez, R. *Organometallics* **2001**, *20*, 2583. (c) Arévalo, S.; de Jesús, E.; de la Mata, F. J.; Flores, J. C.; Gómez, R.; Gómez-Sal, P.; Ortega, P.; Vigo, S. *Organometallics* **2003**, *22*, 5109.

(33) (a) Benito, J. M.; Arévalo, S.; de Jesús, E.; de la Mata, F. J.; Flores, J. C.; Gómez, R. *J. Organomet. Chem.* **2000**, *610*, 42. (b) Benito, J. M.; de Jesús, E.; de la Mata, F. J.; Flores, J. C.; Gómez, R.; Gómez-Sal, P. *J. Organomet. Chem.* **2002**, *664*, 258. (c) Sánchez-Méndez, A.; Silvestri, G. F.; de Jesús, E.; de la Mata, F. J.; Flores, J. C.; Gómez, R.; Gómez-Sal, P. *Eur. J. Inorg. Chem.* **2004**, 3287. (d) Benito, J. M.; de Jesús, E.; de la Mata, F. J.; Flores, J. C.; Gómez, R. *Chem. Commun.* **2005**, 5217.

Scheme 1



2.1–2.3 and 15.6–17.5 for proton and carbon, respectively) and an additional singlet for the pyridinic Me¹⁵ group ($\delta = 2.6$ and 24.4 for proton and carbon, respectively) on going from derivatives **a** to **c**. Another singlet is observed downfield for the imine group (CH⁷, $\delta \approx 8.5$ and 157 for proton and carbon, respectively). This group is also characterized by a strong IR $\nu_{C=N}$ band at ca. 1627 cm^{-1} present in all the derivatives, which appears together with other two intense absorptions in the range 1590–1565 cm^{-1} assigned to the pyridine ring and, in some cases, with a weaker band at ca. 1600 cm^{-1} due to the aromatic C–C vibrations.

The nickel complexes **3a–c** were synthesized by the displacement of the labile ligand in $[\text{NiBr}_2(\text{DME})]$ by the corresponding chelate ligand **2** in dichloromethane (Scheme 1). These compounds are soluble in the reaction solvent and in other polar solvents such as acetone, THF, or acetonitrile, and insoluble in aromatic or aliphatic hydrocarbons. Noteworthy is that their solubility increases with the number of methyl groups on the pyridylimine ligand. The reference complex **3b^{OH}**, accordingly prepared from ligand **1b** (Scheme 1), is found to be slightly soluble in polar solvents. Compound **3b^{OH}** is isolated as a yellow solid and **3a** as an orange solid, whereas **3b** and **3c** are red solids. In the solid state, they can be stored in air without decomposition for unlimited time. However, attempts to crystallize **3a** from ethanol/pentane as a solvent mixture resulted in the protolysis of the Si–O bonds and the redistribution of the ligand, leading to the formation of red crystals of the hexacoordinated complex **4**. This compound was synthesized at a preparative scale by an alternative procedure based on the reaction of 2 equiv of the phenol **1a** as the entering ligand and $[\text{NiBr}_2(\text{DME})]$ in ethanol (Scheme 1). It is known that the formation of bis(chelate)nickel complexes bearing bidentate P/O

ligands is favored in polar solvents,^{13d} and the evolution of mono(P/O) to bis(P/O) nickel compounds by addition of MeOH has been reported recently.^{28a} The NMR spectra of complexes **3** and **4** are not informative because of the interfering effect caused by their paramagnetism. The mass spectrometric data (EI/MS) reveal the molecule ion in the case of complex **3c** and the fragments after the loss of one or two bromide atoms for **3a** and **3c**, together with peaks derived from the bidentate ligand present in each complex. The fragmentation pattern with halide loss has been shown to occur for similar nickel compounds.^{9,10,19a} In all cases the peak isotope distributions match calculated patterns. The positive ion electrospray mass spectra (ESI+/MS) or atmospheric pressure chemical ionization (APCI/MS) of **3a–c**, carried out in acetonitrile solutions, exhibit the fragments after the loss of a bromine atom and coordination of an acetonitrile molecule, whereas in the case of the bis(pyridylimine) compound **4** the coordination of the solvent is not detected and the $[\text{M} - \text{Br}]^+$ fragment is observed. The formation of the $[\text{M} - \text{Br} + \text{solvent}]^+$ ion from related nickel complexes has been described to occur with concomitant appearance in the spectrum of peaks due to dimetallic species formed by halide bridges.³⁴ Compounds **3**, including **3b^{OH}**, also show this behavior. For instance, the APCI/MS spectrum of **3c** dissolved in CH_3CN shows the $[\text{M} - \text{Br} + \text{CH}_3\text{CN}]^+$ peak (m/z 492), together with that corresponding to the dinuclear cation $[\text{M}_2 - \text{Br}]^+$ (m/z 982), and the bis(chelate)metal ion $[(2\text{c})_2\text{NiBr}]^+$ (m/z 763) probably derived from the bis(chelate) dibromonickel complex produced by the addition of the polar solvent.

(34) (a) Sun, W.-H.; Zhang, W.; Gao, T.; Tang, X.; Chen, L.; Li, Y.; Jin, X. *J. Organomet. Chem.* **2004**, 689, 917. (b) Wilson, S. R.; Wu, Y. *Organometallics* **1993**, 12, 1478.

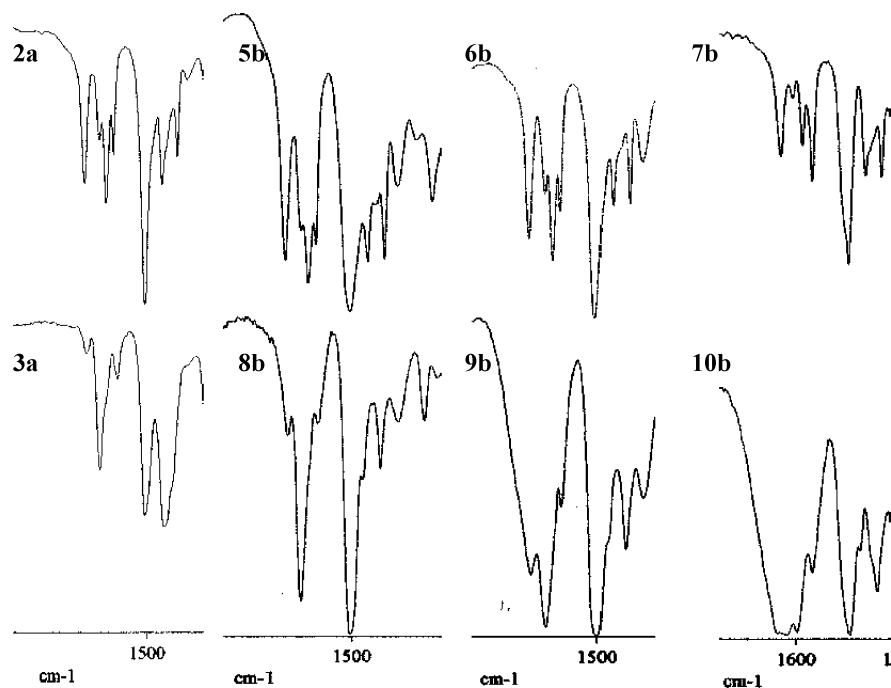


Figure 2. Partial IR spectra of the model ligand **2a**, the dendritic ligands **5b**, **6b**, and **7b** (top), and their corresponding mono- (**3a**) and polymetallic (**8b**–**10b**) nickel complexes (bottom).

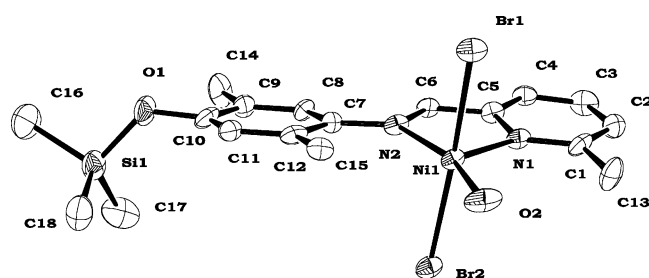


Figure 3. ORTEP diagram of the adduct **3c**·**H**₂**O**.

The IR spectra of compounds **3** and **4** show a single strong absorption at ca. 1589–1596 cm^{-1} , together with two much weaker bands, instead of the group of three intense absorptions observed in the range 1565–1627 cm^{-1} for the imine and pyridine groups in the free ligands (Figure 2). The disappearance or shift of the C=N vibration in the IR spectra of related complexes is explained as a result of the bonding of the pyridylimine ligand to the metal center, reducing the electron density in the C=N bond and, consequently, leading to a lower $\nu_{\text{C=N}}$ value.^{18c}

Molecular Structures of Compounds 3c and 4. The molecular structure of mono(chelate) **3c** and bis(chelate) **4** nickel compounds has been determined by single-crystal X-ray diffraction studies. Figures 3 and 4 show their ORTEP representations, while Tables 1 and 2 summarize relevant structural data.

Complex **3c** crystallized from a solution in wet CH_2Cl_2 . Therefore, one H_2O molecule is coordinated to the metal center in order to compensate the electron deficit of the complex. Increased coordination numbers (i.e., 5 or 6) are commonly found in the solid state for nickel(II) compounds of this type, achieved by bonding to donor ligands (e.g., H_2O , MeCN) or halide bridging, leading to dimeric structures.^{17b,c,34,35} The molecular structure of **3c** consists of discrete molecules, with a five-coordinated nickel center. The coordination polyhedra can be regarded as a slightly deformed trigonal bipyramid in which the equatorial plane includes the nitrogen atoms of the chelating ligand and the oxygen atom of the coordinated H_2O . The

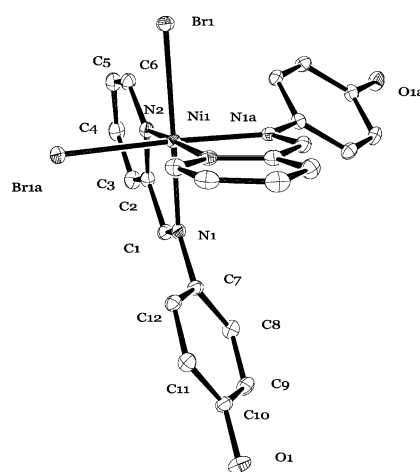
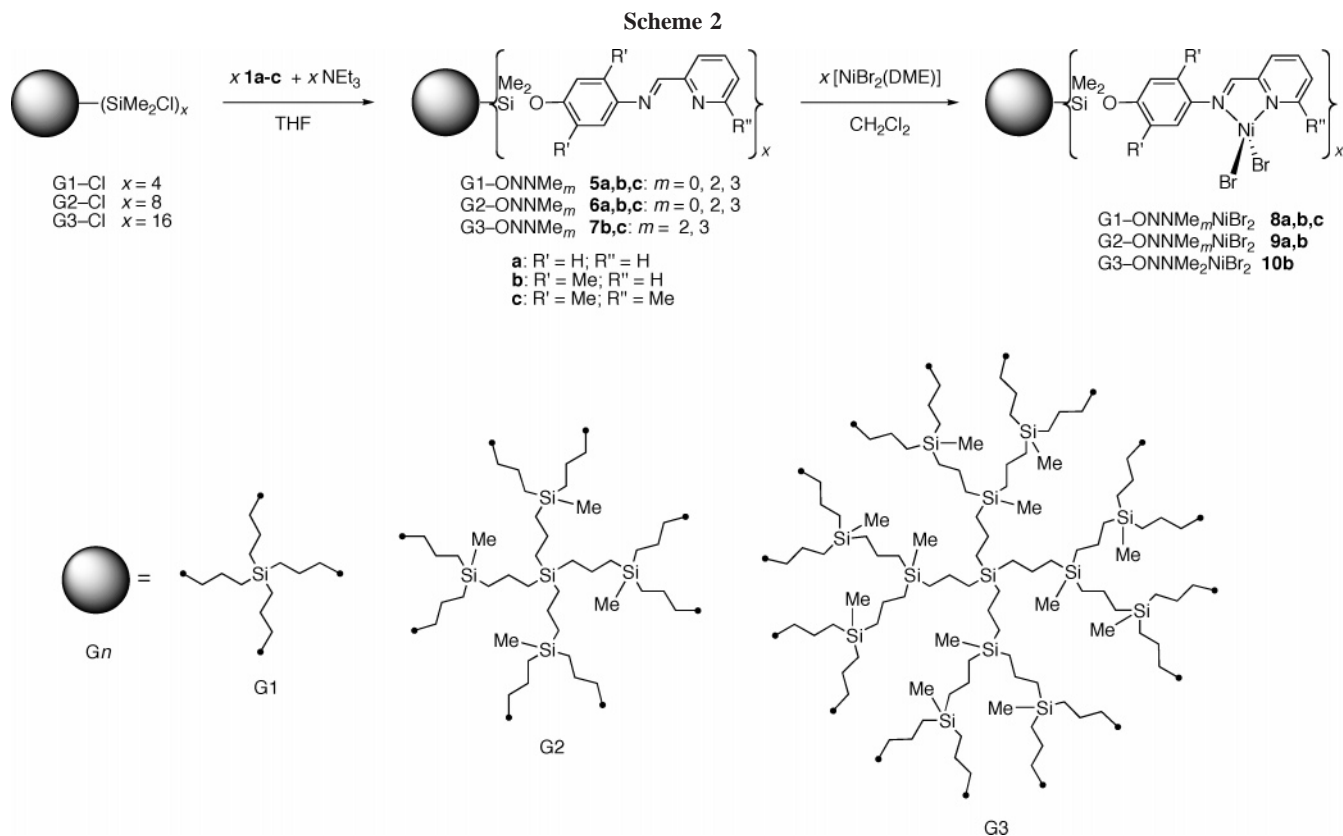


Figure 4. ORTEP drawing of enantiomer Δ of compound **4**.

Table 1. Selected Bond Distances (Å) and Angles (deg) for **3c**·**H**₂**O**

Bond Distances			
N(2)–Ni(1)	2.056(6)	Br(2)–Ni(1)	2.5009(16)
N(1)–Ni(1)	2.028(7)	N(2)–C(6)	1.285(10)
Ni(1)–O(2)	2.013(5)	C(6)–C(5)	1.449(11)
Br(1)–Ni(1)	2.5384(17)	N(1)–C(5)	1.373(8)
C(7)–N(2)	1.425(10)		
C(12)–C(15)	1.508(10)		
C(1)–C(13)	1.510(10)		
Bond Angles			
N(1)–Ni(1)–N(2)	82.2(3)	Br(1)–Ni(1)–O(2)	85.5(2)
N(2)–Ni(1)–O(2)	160.5(3)	Br(2)–Ni(1)–O(2)	87.5(2)
O(2)–Ni(1)–N(1)	117.3(3)	C(7)–N(2)–C(6)	120.6(6)
Br(1)–Ni(1)–N(2)	95.53(19)	Si(1)–O(1)–C(10)	127.4(6)
Br(1)–Ni(1)–N(1)	90.5(2)	N(1)–C(1)–C(13)	116.7(8)
Br(1)–Ni(1)–Br(2)	171.14(5)		

bromine atoms occupy the axial coordination sites and are somewhat tilted from the perpendicular position to the equatorial plane, toward the H_2O molecule, due to the steric repulsion between the large bromine substituents and the pyridylimine ligand. The positioning of the coordinated H_2O is asymmetrical with the respect to the chelate ligand, being closer to the pyridine donor atom (bond angle O(2)–Ni(1)–N(1) = 117.3°) and almost *trans* to the imine group (O(2)–Ni(1)–N(2) = 160.5-

**Table 2. Selected Bond Distances (Å) and Angles (deg) for Complex 4**

Bond Distances					
Ni(1)–Br(1)	2.5930(3)	Ni(1)–N(1)	2.1387(14)	N(1)–C(1)	1.288(2)
Ni(1)–Br(1a) ^a	2.5930(3)	O(1)–C(10)	1.363(2)	C(1)–C(2)	1.459(2)
Ni(1)–N(2)	2.0833(14)	N(1)–C(7)	1.428(2)	C(2)–N(2)	1.352(2)
Bond Angles					
N(1)–Ni(1)–N(2)	78.62(5)	N(2)–Ni(1)–Br(1a) ^a		88.26(4)	
N(1)–Ni(1)–N(2a) ^a	98.24(5)	N(2)–Ni(1)–N(2a) ^a		175.70(8)	
N(1a)–Ni(1)–N(2) ^a	98.24(5)	N(1)–Ni(1)–Br(1)		173.32(4)	
N(1)–Ni(1)–N(1a) ^a	88.06(7)	N(1)–Ni(1)–Br(1a) ^a		91.70(4)	
Br(1)–Ni(1)–N(2)	94.81(4)	Br(1)–Ni(1)–Br(1a) ^a		89.30(1)	

^a Symmetry transformations used to generate equivalent atoms a: $-x, y, -z+1/2$.

(3)^o. Worth mentioning is that the aryl ring lies nearly on the plane formed by the metal, the imine nitrogen, and the pyridine ring (torsion angle C(8)–C(7)–N(2)–C(6) = 9.5^o), whereas in related complexes with dimeric structure, as two bridging bromine atoms connect the metal centers, the phenyl ring adopts a position close to perpendicular to the pyridine ring.^{17c} The distances N(2)–C(6) and C(6)–C(5) are indicative of localization of the imine double bond.

Complex **4** crystallized by slow diffusion of a pentane layer into a concentrated solution in ethanol. The asymmetric part of the unit cell consists of half of the molecule and a crystallization H₂O molecule, and the whole molecule is formed by two halves related by a binary axis. The nickel atom is a six-coordinated center with a distorted octahedral geometry, with two bromine atoms and two N/N chelating ligands. Although the coordination number 6 is frequent in nickel chemistry, a small number of bis(pyridylimine) octahedral compounds are known so far.³⁶ The positioning of the ligands around the metal center in compound **4** follows the maximum hardness principle (MHP), and therefore, the hardest ligand (imine) is in *trans* position to the softest one (bromo).³⁷ Figure 4 depicts enantiomer Δ , although the two possible enantiomers are present in the unit cell. In this case

and compared to the structure of **3c**, the aryl groups are rotated with respect to the N–Ni–py plane (torsion angle C(1)–N(1)–C(7)–C(8) = 41.7^o) and are substituted by hydroxy instead of siloxy groups.

Synthesis and Characterization of Dendrimers. The pyridylimine ligands described above have been used as linkers between carborane dendrimers and metal complexes. Thus, the methodology applied for the preparation of ligands **2** and metal complexes **3** has been extended to synthesize G1-ONNMe_m (**5**), G2-ONNMe_m (**6**), G3-ONNMe_m (**7**), and their polymetallic nickel derivatives (**8–10**, Scheme 2, Figure 5).

Dendritic ligands G1-ONNMe_m (**5a**, $m = 0$; **5b**, $m = 2$; **5c**, $m = 3$), G2-ONNMe_m (**6a**, $m = 0$; **6b**, $m = 2$; **6c**, $m = 3$), and G3-ONNMe_m (**7b**, $m = 2$; **7c**, $m = 3$) were obtained by phenolysis of the terminal silyl-chloride groups in carboranes G1–Cl, G2–Cl, and G3–Cl,³⁸ with pyridylimines **1a–c** in the presence of NEt₃ in THF. After workup, they were isolated in good yield as yellow (**5a–c**) or brownish (**6a–c** and **7b,c**) viscous oils. Their solubility increases with the number of methyl groups on the pyridylimine ligand and diminishes with the increase of dendrimer generation. MALDI-TOF mass spectra carried out for **5b,c** and **6b,c**, using dithranol as a matrix, show the protonated parent peak $[M + H]^+$. The complete substitution of the chloride atom at the end of the branches in the starting dendrimers Gn-Cl by pyridylimine groups in **5–7** was confirmed

(35) (a) Jie, S.; Zhang, D.; Zhang, T.; Sun, W.-H.; Chen, J.; Ren, Q.; Liu, D.; Zheng, G.; Chen, W. *J. Organomet. Chem.* **2005**, *690*, 1739. (b) Tang, X.; Sun, W.-H.; Gao, T.; Hou, J.; Chen, J.; Chen, W. *J. Organomet. Chem.* **2005**, *690*, 1570. (c) Britovsek, G. J. P.; Baugh, S. P. D.; Hoarau, O.; Gibson, V. C.; Wass, D. F.; White, A. J. P.; Williams, D. J. *Inorg. Chim. Acta* **2003**, *345*, 279.

(36) (a) Garoufis, A.; Kasselouri, S.; Raptopoulou, C. P.; Terzis, A. *Polyhedron* **1999**, *18*, 585. (b) Riggall, K.; Lynde-Kernell, T.; Schlemper, E. O. *J. Coord. Chem.* **1992**, *25*, 117.

(37) (a) Pearson, R. G. *J. Chem. Edu.* **1999**, *76*, 267. (b) Arnaiz, A.; Garcia-Herbosa, G.; Cuevas, J. V.; Lavastre, O.; Hillairet, C.; Toupet, L. *Collect. Czech. Chem. Commun.* **2002**, *67*, 1200.

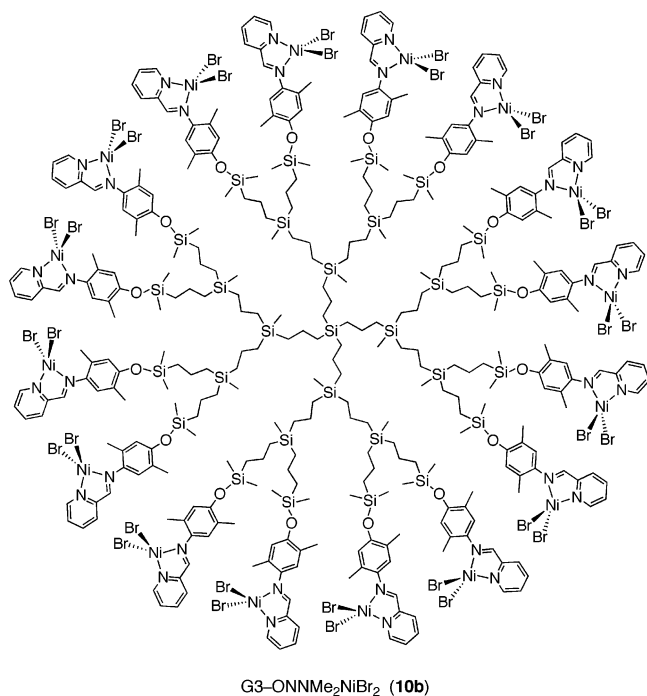


Figure 5. Metallodendrimer **10b**.

by ^1H and $^{13}\text{C}\{^1\text{H}\}$ NMR. $^{29}\text{Si}\{^1\text{H}\}$ NMR spectra show a singlet for every generation silicon nuclei with chemical shifts almost insensitive to the dendrimer generation and to the pyridylimine group substitution: δ 18–19 for the SiMe_2 groups and 0–1 for the central Si atom and the inner SiMe groups. The IR spectra of all dendritic ligands **5–7** show the characteristic group of three intense absorptions mentioned above for the imine group and the pyridine ring (for examples see Figure 3).

Dendrimers **5–7** are useful supports to coordinate 4, 8, or 16 metal centers through the asymmetrical N/N bidentate terminal groups (Scheme 2, Figure 5). Thus, reactions with $[\text{NiBr}_2(\text{DME})]$ in CH_2Cl_2 led to the formation of metallodendrimers **8–10**, which were isolated as mustard-yellow or orange paramagnetic air-stable solids that can be stored in conventional vials exposed to air without decomposition. They are only slightly soluble in solvents such as CH_2Cl_2 or THF, and again, their solubility increases with the number of methyl substituents on the pyridylimine group and decreases with the generation number of the dendrimer. The solubility is a relevant fact since low solubilities severely limit the preparation of high-generation dendrimers.

The paramagnetism of nickel dendrimers **8–10** makes ineffective their characterization by NMR studies. They were characterized by elemental analysis and IR. Mass spectrometry was only informative in the case of G1-ONNMe₃NiBr₂ (**8c**), which was soluble enough in CH_2Cl_2 to allow the formation of a solid sample in a dithranol matrix by evaporation. The MALDI-TOF mass spectrum from that sample exhibits a peak at $m/z = 2180.3$ corresponding to the $[\text{M} - \text{Br}]^+$ fragment, the cation after the loss of only one of the eight bromine atoms present. The IR spectra of all metallodendrimers **8–10** are also consistent with coordination of the pyridylimine groups, showing a strong absorption at ca. 1597 cm^{-1} , together two weaker bands, instead of the group of three intense absorptions observed in

the range $1565\text{--}1627\text{ cm}^{-1}$ for the corresponding free dendritic ligand (representative examples in Figure 3).

Ethylene Catalyses Using Pyridylimine Nickel Compounds. Nickel monometallic (**3**, **4**) and dendritic compounds (**8–10**) were activated using MAO and screened for ethylene catalysis under the same mild conditions and concentration of nickel centers. The nickel compounds combined with the cocatalyst became readily soluble in toluene, and we found the starting material $[\text{NiBr}_2(\text{DME})]$ to be totally inactive under the same reaction conditions. The catalytic results are summarized in Table 3.

As shown in the table, roughly all catalysts gave a toluene-soluble fraction of oligomers together with solid polyethylene (PE), with low to moderate activities according to Gibson's classification.³⁹ The oligomeric oily products are mainly composed of even olefins up to C_{34} , with number average molecular weight in the range $M_n = 220\text{--}370$, and they are characterized by Schulz–Flory chain length distributions with α values from 0.45 to 0.70 ($\alpha = k_p/(k_p + k_{ct}) = \text{mol of } \text{C}_{n+2}/\text{mol of } \text{C}_n$; k_p = rate of propagation, k_{ct} = rate of chain transfer).⁴⁰ Small amounts of even alkanes (<5 wt %) are also detected in the GC analysis, which is consistent with the occurrence of chain transfer to “free” trimethylaluminum present in the MAO solution used as cocatalyst.^{41,42} Among the olefinic products obtained, the selectivity in α -olefins is between 45 and 65 mol %, and the remainder are almost exclusively 2-alkenes (*cis*- and *trans*- $\text{CH}_3\text{CH}=\text{CHR}$). This observation, together with the relatively low branching observed by ^1H NMR (3–5 branches per 100 C, for C_4 to C_{34} oligomers),^{16b,c} indicates that chain walking of the oligomerization-active species proceeds, in most cases, as much to the β -carbon under these experimental conditions.

A much higher degree of branching is found in the solid polymers. Some of them are as densely branched as PE polymers prepared from palladium-diimine catalysts under comparable conditions, and considered hyperbranched.⁴³ It is noteworthy that the later class of catalysts produces from linear to dendritic PE by tuning the ethylene pressure or the substitution on the ancillary ligand.⁴⁴ T_m values of all samples (116–125 °C, Table 3) are in agreement with their level of chain branching and are lower than those typically found for HDPE (≥ 135 °C). GPC analysis of the solid materials shows that the weight average molecular weights are low ($M_w = 1600\text{--}177\,000$) with wide distributions (PDI = 3–20). The quantitative ^{13}C NMR analyses of the polymers formed (a representative spectrum is shown in Figure 6) show branching densities in the range of 60–170 total branches per 1000 main-chain carbons (Table 3), and according to Galland et al.,⁴⁵ an abundant amount of branches are relatively long (≥ 6 C). In addition, all peaks in the carbon-13 spectra

(39) Britovsek, G. J. P.; Gibson, V. C.; Wass, D. F. *Angew. Chem., Int. Ed.* **1999**, *38*, 428.

(40) (a) Schulz, G. V. *Z. Phys. Chem., Abt. B* **1935**, *30*, 379. (b) Flory, P. J. *J. Am. Chem. Soc.* **1940**, *62*, 1561.

(41) (a) Small, B. L.; Brookhart, M.; Bennett, A. M. A. *J. Am. Chem. Soc.* **1998**, *120*, 4049. (b) Chen, Y.; Chen, R.; Qian, C.; Dong, X.; Sun, J. *Organometallics* **2003**, *22*, 4312. (c) Britovsek, G. J. P.; Cohen, S. A.; Gibson, V. C.; van Meurs, M. *J. Am. Chem. Soc.* **2004**, *126*, 10701.

(42) Even PMAO-IP (polymethylaluminumoxane, improved process), commercialized by Akzo-Nobel, is known to contain some residual TEA. For instance see: Busico, V.; Cipullo, R.; Cuttillo, F.; Friederichs, N.; Ronca, S.; Wang, B. *J. Am. Chem. Soc.* **2003**, *125*, 12402.

(43) Cotts, M. P.; Guan, Z.; McCord, E.; McLain, S. *Macromolecules* **2000**, *19*, 6945.

(44) (a) Popeney, C.; Guan, Z. *Organometallics* **2005**, *24*, 1145. (b) Chen, G.; Guan, Z. *J. Am. Chem. Soc.* **2004**, *126*, 2662. (c) Guan, Z. *Chem. Eur. J.* **2002**, *8*, 3087. (d) Guan, Z.; Cotts, P. M.; McCord, E. F.; McLain, S. J. *Science* **1999**, *283*, 2059.

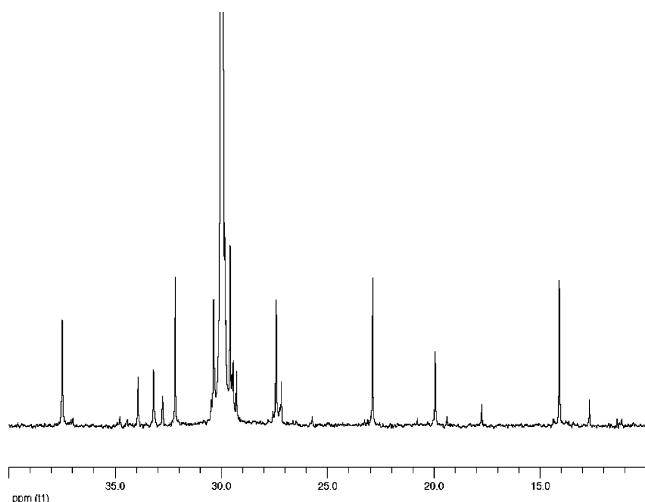
(45) Galland, G. B.; de Souza, R. F.; Mauler, R. S.; Nunes, F. F. *Macromolecules* **1999**, *32*, 1620.

(38) (a) van der Made, A. W.; van Leeuwen, P. W. N. M. *J. Chem. Soc., Chem. Commun.* **1992**, 1400. (b) Alonso, B.; Cuadrado, I.; Morán, M.; Losada, J. *J. Chem. Soc., Chem. Commun.* **1994**, 2575. (c) Seyferth, D.; Kugita, T.; Rheingold, A. L.; Yap, G. P. A. *Organometallics* **1995**, *14*, 5362.

Table 3. Ethylene Oligomerization/Polymerization Catalyzed by Monometallic and Dendritic Pyridylimine Nickel Precursors^a

entry	precatalyst	oligomers					polymer						
		oligomer TOF ^{b,c} (h ⁻¹)	$\alpha^{d,e}$	α -olefin (mol %) ^e	M_n^f	branches/100 C ^g	polymer yield (g)	polymer TOF ^b (h ⁻¹)	T_m (°C) ^h	C_n branches/1000 C ⁱ n = 1/2–5/≥6	10 ⁻³ M_w^j	PDI ^j	
1	3a	240	0.63	66	219.6	3	0.30	32	120.3	12/24/80	116	2.75	2.74
2	3b	372	0.70	48	265.8	3	8.90	944	117.1	12/36/97	145	1.64	5.58
3	3c	traces ^k					0.08	8	121.4	66/41/64	171	6.01	4.19
4	3b^{OH}	264	0.65	45	341.1	4	1.40	149	122.0	10/18/48	76	5.88	6.61
5	4	traces ^k					0.05	5	121.4	n.d. ^l	n.d. ^l	11.32	11.35
6	8a (G1-ONNNiBr ₂)	293	0.67	60	286.1	3	0.07	7	119.6	11/21/56	88	27.89	20.12
7	9a (G2-ONNNiBr ₂)	306	0.61	62	371.9	5	0.20	21	121.3	15/10/34	59	177.04	2.84
8	8b (G1-ONNMe ₂ NiBr ₂)	594	0.60	55	284.5	3	10.02	1063	120.5	17/22/62	101	2.16	2.77
9	9b (G2-ONNMe ₂ NiBr ₂)	729	0.51	46	342.5	3	3.45	366	123.2	13/11/38	62	10.62	11.25
10	10b (G3-ONNMe ₂ NiBr ₂)	957	0.45	45	327.6	3	3.24	344	124.7	12/10/36	58	17.07	14.06
11	8c (G1-ONNMe ₃ NiBr ₂)	traces ^k					0.02	2	119.0	4/35/19	58	n.d. ^l	n.d. ^l

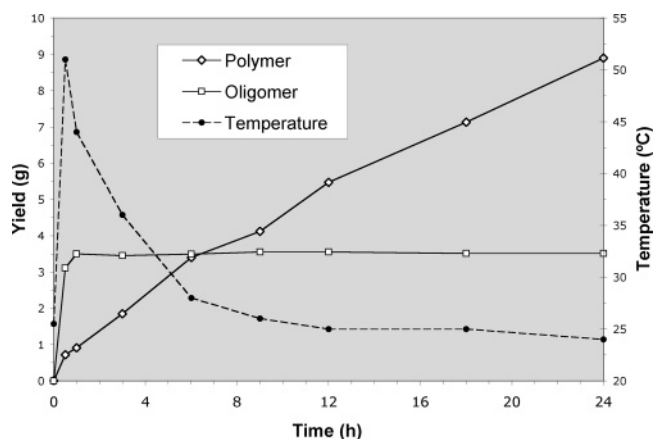
^aPolymerization conditions: 50 mL of toluene; $n(\text{Ni}) = 14 \mu\text{mol}$; Al/Ni = 1000; $t_p = 24 \text{ h}$; $T_p = 20 \text{ °C}$; $\text{PC}_2\text{H}_4 = 2 \text{ bar}$; activities $\pm 7\%$. ^b Turnover frequency: mol of C_2H_4 converted/(mol_{Ni} × h). ^c Corrected to consider the lower olefin lost during workup. ^d Schulz–Flory parameter, $\alpha = \text{rate of propagation} / (\text{rate of propagation} + \text{rate of chain transfer})$.⁴⁰ ^e Determined by GC. ^f Determined by ¹H NMR.^{16b,c} ^g Total number of methyl per 100 C. ^h Determined by DSC (second heating run). ⁱ Determined by ¹³C NMR.⁴⁵ ^j Determined by GPC. ^k Less than 3 mg of very impure oligomers. ^l Not determined.

**Figure 6.** ¹³C NMR spectrum of PE made using catalyst **8b**.

were assigned except two low-intensity resonances (δ 17.7 and 12.7), which are believed to be due to a branch-on-branch structure.⁴³ These findings imply that polymerization-active species walk along the chain much further than the oligomerization ones.

Although oligomers and polymers might be formed by the same or by two different active centers, the latter is more feasible. It has been recently shown that C_1 symmetry precursors lead simultaneously to PE or oligomeric products depending on the catalytic face where alkyl propagation takes place.⁴⁶ This could be the case for compound **3b** and related metallodendrimers **8b–10b**, with a hindered rotation of the aryl group about the C–N bond. However the parent compound **3a** is a C_s symmetric precursor and behaves similarly, producing α -olefins and polymer.

Moreover, these active species seem to have different lifetimes. Figure 7 illustrates the variation of yields and temperature over a 24 h period using **3b**; similar profiles are observed for the other mono- and polymetallic precursors. The data reveal that almost 90% of the oligomers are already formed 30 min after the reaction start, coinciding with the exotherm maximum, whereas the polymerization-active species show long lifetimes under these conditions, with low loss of activity over the period studied.

**Figure 7.** Variation with time of T_p and yield of PE and oligomers produced by **3b**.

The production of oligomers and polymers by eventual formation of bis(pyridylimine)nickel species or splitting of the Si–O bond by the addition of the cocatalysts is excluded because of the observed performances of compounds **3b^{OH}** and **4** (entries 4 and 5, Table 3). The latter is scarcely active, and the former also gives the two types of ethylene products, although behaving differently than **3b** and related dendrimers. Therefore, protection at the phenolic oxygen, even with a very simple carbosilane group (SiMe_3), seems to be positive in terms of polymerization activity (compare the performance of **3b^{OH}** vs **3b**), and the presence of a second chelate ligand deactivates the metal center probably by saturation of the coordination sphere (compare **4** vs **3b^{OH}**).

The effect on the catalytic behavior of the methyl substituent in the 6-position of the ligand pyridine ring in compounds **c** (**3c** and **8c**) concurs with earlier findings.^{17c,19a} Thus, the activities in oligomerization or polymerization for both compounds are almost negligible as a result of steric obstruction exerted by the methyl group pointing to the equatorial coordination sites. On the other hand, it is well established that ligand substitution on the *ortho* aryl positions produces a steric protection of the axial coordination sites, which has a profound effect on the catalytic activity of this type of precursors and on the properties of the catalytic products.^{1–3} Furthermore, it has been described that catalysts without enough steric bulk in those *ortho* positions of the pyridylimine ligand are more easily deactivated through the interaction with the alkylaluminum

(46) Bianchini, C.; Giambastiani, G.; Guerrero, I. R.; Meli, A.; Passaglia, E.; Gragnoli, T. *Organometallics* **2004**, *23*, 6087.

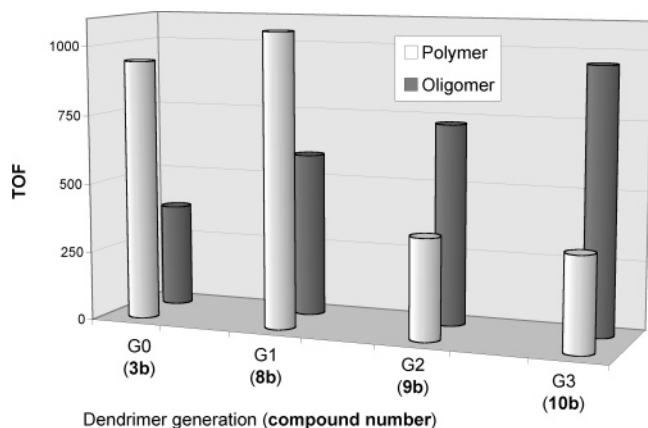


Figure 8. Turnover frequencies (mol of C₂H₄ converted × mol_{Ni}⁻¹ × h⁻¹) producing oligomers and polymers by *Gn*-ONNMe₂NiBr₂ under the conditions described in Table 3.

cocatalyst.⁴⁷ The data summarized in Table 3 are in agreement with these remarks and show a trend in activity: compounds **b** > **a** > **c**. Compounds **3a**, **8a**, and **9a** show oligomerization turnover frequencies slightly inferior and polymerization activities much lower than those corresponding to **3b**, **8b**, and **9b**. In general, the selectivity for α -olefins is higher for the nonsubstituted catalysts **a**, whereas substituted compounds **b** give rise to more branched polymers, with lower molecular weights.

Several trends arise when analyzing the data in Table 3 with regard to the metallic nuclearity or generation of the precursors. The activity leading to oligomers slightly increases (see entries 1, 6, and 7 for precatalysts **a** and entries 2, 8, 9, and 10 for **b**), whereas the activity producing polymer diminishes for higher generations (see corresponding entries for the **a**, **b**, and **c** series in Table 3). For instance, Figure 8 depicts turnover frequencies in the production of polymer and oligomer with precursors **b** (**3b**, **8b**, **9b**, and **10b**) under the same reaction conditions. It is shown that monometallic compound **3b** is superior, yielding PE rather than oligomer, while the contrary is observed for polynuclear dendrimer **10b**, with 16 Ni centers. The Schulz–Flory parameter (α) for the most active compounds **b** also decreases with increasing nuclearity. Conversely, higher molecular weights (and PDIs) are generally observed for polymers produced by higher generations. The branching degree of the polymers is also generation-dependent and decreases progressively. For instance, it drops from 145 for the monometallic complex **3b** to 58 branches per 1000 C for G3 dendrimer **10b**; this reduction in the number of branches is larger for the longest branches than for methyl ones.

These results might be interpreted as a consequence of the combination of the “steric pressure” on the growing chains and “microenvironment protection” of higher generation dendrimers on the polymerization species. Their bulkiness enhances chain transfer processes and favors the performance of the oligomerization species, as reflected by a decrease in the α parameter and an increase in activity, respectively. A larger size also affects the polymerization-active species, preventing the catalyst chain-walking process from going too deep into the coiled polymer chain (see Figure 9), leading to less branched polymers. At the same time, the polymers are probably produced by more protected active centers in larger dendrimers, with lower activity, but higher M_w (and PDI). For instance, the latter is reasonable if back-folding of terminal active species into the dendrimer matrix becomes significant at higher generation.

Conclusions

In summary, the carbosilane dendrimers containing peripheral pyridylimine groups reported herein represent a new set of versatile dendritic ligands that have been used for the preparation of new nickel metallodendrimers. Upon activation with MAO under mild conditions, the nickel derivatives are active for ethylene oligomerization and polymerization, and their catalytic properties are definitely sensitive to the ligand structure and the dendrimer generation. Although the precise nature of the active species for each type of insertion product remains elusive to date, significant ligand and dendrimer effects have emerged. Steric protection of axial coordination sites by methyl substituents on the aryl ring increases the activities for both oligomers and polyethylene. However, the presence of a methyl group on the 6-position of the pyridine moiety, hindering the equatorial coordination sites, causes the reverse. The size of the dendrimer regulates the production of ethylene insertion products (oligomer vs polymer), the oligomer chain-length distribution (α), and the branching density, molecular weight, and polydispersity of the polymers. These findings may be useful for controlling the structure/properties of ethylene insertion products.

When the pioneering work on dendrimer-bound metal catalysts was published in 1994, it was remarked that such systems had the adequate shape and size to be removed from the solution of products using nanofiltration methods, at the same time retaining the characteristics found for the monomeric model.⁴⁸ If the metal centers are directly available for the substrate in the periphery-type of dendrimeric catalysts, as in mononuclear homogeneous catalysts, then comparable activities and selectivities are expected for both systems. However, dendritic effects

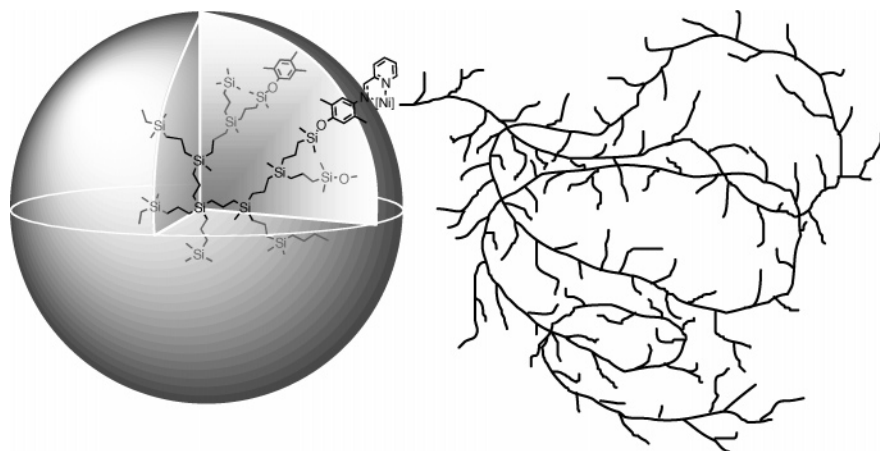


Figure 9. Representation of a branched polyethylene chain growing at the dendrimer periphery.

on activity, both positive and negative, or selectivity have been observed and ascribed to the proximity of active sites and steric crowding on the surface of the dendrimers.⁴⁹ Whereas catalyst recycling plays a central role with palladium and other rare catalysts, oligomerization/polymerization of olefins with dendrimers can benefit from improvements in the stability of active species or in the control of the microstructure, molecular weight, or stereochemistry of the polymers. Recently, the activity of a (P,O)nickel complex has been improved by embedding such a catalyst in a dendritic framework, which restricts the formation of inactive bis(P,O)nickel complexes.^{30a} In this paper we have shown an example in which the size of the dendrimer regulates the characteristics of ethylene insertion products. It is noteworthy that this dendritic effect has been obtained with peripheral metal dendrimers when core or focal-point dendrimers are a priori more suited systems for these purposes.

Experimental Section

Reagents and General Techniques. All operations were performed under an argon atmosphere using Schlenk or drybox techniques. Unless otherwise stated, reagents were obtained from commercial sources and used as received. [NiBr₂(DME)],⁵⁰ and carbosilane dendrimers *Gn*-Cl (*n* = 1, 2, 3)³⁸ were prepared according to literature procedures. Solvents were previously dried prior to use and distilled under argon as described elsewhere.⁵¹ NMR spectra were recorded on Varian Unity 500+, Varian Unity VR-300, or Varian Unity 200 NMR spectrometers. Chemical shifts (δ) are reported in ppm referenced to SiMe₄ for ¹H, ¹³C, and ²⁹Si, and assignments for the iminopyridyl ligands are according to the numbering scheme depicted in Figure 1. IR spectra were recorded on a Perkin-Elmer FT-IR Spectrum-2000 spectrophotometer. Elemental analyses and mass spectra were performed by the Microanalytical Laboratories of the University of Alcalá (MLUAH) on a Heraeus CHN-O-Rapid microanalyzer and on a Hewlett-Packard 5988A Quadrupole (EI) or a Thermo Quest Finnigan Automass Multi (ESI) mass spectrometer. MALDI-TOF MS were performed by the Analytical Services of the Universidad Autónoma de Madrid in a Bruker Reflex II spectrometer, using samples in a 1,8,9-trihydroxyanthracene (dithranol) matrix. Polymethylaluminoxane improved process (PMAO-IP) in toluene (13 wt % Al) was purchased from Akzo Nobel. Oligomer products were analyzed on a Chrompack CP 9001 gas chromatograph using a CP-Sil 5CB capillary column (10 m, 0.25 mm i.d., 0.12 μ m df) under the following conditions: injector and detector temperature, 250 °C; oven temperature program, 100 °C/5 min, 5 °C/min ramp, 250 °C/15 min. DSC melting endotherms of polymers were performed on a Perkin-Elmer DSC 6 instrument. Polyethylene molecular weight determinations were made by MLUAH on a Waters GPCV 2000

(47) Britovsek, G. J. P.; Mastroianni, S.; Solan, G. A.; Baugh, S. P. D.; Redshaw, C.; Gibson, V. C.; White, A. J. P.; Williams, D. J.; Elsegood, M. R. *J. Chem. Eur. J.* **2000**, *6*, 2221.

(48) Knapen, J. W. J.; van der Made, A. W.; de Wilde, J. C.; van Leeuwen, P. W. N. M.; Wijkens, P.; Grove, D. M.; van Koten, G. *Nature* **1994**, *372*, 659.

(49) (a) Mizugaki, T.; Ooe, M.; Ebitani, K.; Kaneda, K. *J. Mol. Catal. A: Chem.* **1999**, *145*, 329. (b) Kleij, A. W.; Gossage, R. A.; Jastrzebski, J. T. B. H.; Boersma, J.; van Koten, G. *Angew. Chem., Int. Ed.* **2000**, *39*, 176. (c) Breinbauer, R.; Jacobsen, E. N. *Angew. Chem., Int. Ed.* **2000**, *39*, 3604. (d) Kleij, A. W.; Gossage, R. A.; Gebbink, R. J. M. K.; Brinkmann, N.; Reijerse, E. J.; Kragl, U.; Lutz, M.; Spek, A. L.; van Koten, G. *J. Am. Chem. Soc.* **2000**, *122*, 12112. (e) Ropartz, L.; Morris, R. E.; Foster, D. F.; Cole-Hamilton, D. J. *Chem. Commun.* **2001**, 361. (f) Dahan, A.; Portnoy, M. *Chem. Commun.* **2002**, 2700. (g) Drake, M. D.; F. V.; Bright, M. R. *Detty, J. Am. Chem. Soc.* **2003**, *125*, 12558. (h) Delort, E.; Darbre, T.; Reymond, J.-L. *J. Am. Chem. Soc.* **2004**, *126*, 15642.

(50) Ward, L. G. L. In *Inorganic Syntheses*; Cotton, F. A., Ed.; McGraw-Hill: New York, 1972; Vol. 13, p 154.

(51) Perrin, D. P.; Armarego, W. L. F. *Purification of Laboratory Chemicals*, 3rd ed.; Pergamon Press: Oxford, 1988.

operating at 135 °C with 1,2,4-trichlorobenzene (TCB) solvent and polystyrene calibration standards.

Preparation of *N*-(4-Hydroxyphenyl)-2-pyridylmethanimines (1). Compound **1a** was synthesized as described in the literature,^{22a} whereas **1b** and **1c** were synthesized by adapting this procedure as already reported for **1b**.^{33d}

1c. The preparation was similar to that of **1b** but starting from 6-methylpyridine-2-carbaldehyde (0.88 g, 7.3 mmol) and 4-amino-2,5-dimethylphenol (1.00 g, 7.29 mmol). Compound **1c** was found to be soluble in toluene, CH₂Cl₂, and THF and insoluble in hexanes. The yellow solid could be purified by recrystallization from toluene or by sublimation (160 °C, 10⁻³ mmHg). Yield: 1.50 g (86%). Anal. Calc for C₁₅H₁₆N₂O (240.30): C, 74.97; H, 6.71; N, 11.66. Found: C, 74.87; H, 6.72; N, 11.69. ¹H NMR (CDCl₃): δ 2.21 (s, 3H, Me¹⁴), 2.33 (s, 3H, Me¹³), 2.62 (s, 3H, Me¹⁵), 5.16 (br s, 1H, OH), 6.64 (s, 1H, H³), 6.90 (s, 1H, H⁶), 7.19 (d, 1H, *J*_{H,H} = 7.5 Hz, H¹¹), 7.66 (pt, 1H, H¹⁰), 8.03 (d, 1H, *J*_{H,H} = 7.7 Hz, H⁹), 8.48 (s, 1H, H⁷). ¹³C{¹H} NMR (CDCl₃): δ 15.6 and 17.5 (Me^{13,14}), 24.4 (Me¹⁵), 116.8 (C³), 118.4 (C⁶), 119.8 (C⁹), 121.8 (C⁵), 124.3 (C¹¹), 132.4 (C²), 136.8 (C¹⁰), 142.5 (C¹), 152.7 (C⁴), 154.6 (C⁸), 157.6 (C⁷) 158.0 (C¹²). IR (KBr): ν 1620 cm⁻¹ (s, C=N), 1607 (w, C=C), 1594 and 1573 cm⁻¹ (s and vs, py-ring). MS (70 eV, EI): *m/z* 240 [M]⁺.

Preparation of *N*-(4-Trimethylsilyloxyphenyl)-2-pyridylmethanimines (2). Compounds **2a–c** were prepared in high yields (80–90%), starting from the corresponding pyridylimine **1**, as described previously for **2a**^{22a} and **2b**.^{33d} The former was alternatively synthesized as follows.

2a. 4-Trimethylsilyloxyaniline (0.80 g, 4.4 mmol),^{33a} pyridine-2-carbaldehyde (0.48 g, 4.5 mmol), MgSO₄ (5 g), and ethyl acetate (60 mL) were heated under reflux for 2 h and then stirred overnight at room temperature. The solvent was removed under reduced pressure, and the residue extracted with diethyl ether (2 \times 30 mL). Removal of the ether afforded spectroscopically pure **2a** as an orange-yellow oil, soluble in all common organic solvents. Yield: 0.95 g (80%).

2c: orange-yellow oil. Yield: 91%. Anal. Calc for C₁₈H₂₄N₂-OSi (312.49): C, 69.19; H, 7.74; N, 8.96. Found: C, 68.93; H, 7.66; N, 8.87. ¹H NMR (CDCl₃): δ 0.26 (s, 9H, SiMe₃), 2.14 (s, 3H, Me¹⁴), 2.34 (s, 3H, Me¹³), 2.60 (s, 3H, Me¹⁵), 6.63 (s, 1H, H³), 6.92 (s, 1H, H⁶), 7.17 (d, 1H, *J*_{H,H} = 7.7, H¹¹), 7.65 (pt, 1H, H¹⁰), 8.03 (d, 1H, *J*_{H,H} = 7.7 Hz, H⁹), 8.49 (s, 1H, H⁷). ¹³C{¹H} NMR (CDCl₃): δ 0.6 (SiMe₃), 16.3 and 17.6 (Me^{13,14}), 24.4 (Me¹⁵), 118.3 (C³), 119.7 (C⁶), 120.7 (C⁹), 124.2 (C¹¹), 126.8 (C⁵), 131.6 (C²), 136.6 (C¹⁰), 142.9 (C¹), 152.4 (C⁴), 154.6 (C⁸), 157.7 (C⁷), 158.0 (C¹²). ²⁹Si{¹H} NMR (CDCl₃): δ 18.9 (SiMe₃). IR (Nujol/CsI): ν 1627 cm⁻¹ (s, C=N), 1589 and 1572 cm⁻¹ (s, py-ring). MS (70 eV, EI): *m/z* 313 [M]⁺.

Preparation of Nickel Complexes (3, 4). The synthesis of the nickel compounds **3a–c** is exemplified by the preparation of **3a**. The syntheses of compounds **3b** and **3b**^{OH} have been reported in a preliminary communication.^{33d}

NiBr₂(Me₃SiO-4-Ph-N=CH-2-Py) (3a). Ligand **2a** (1.18 g, 4.36 mmol), [NiBr₂(DME)] (1.34 g, 4.34 mmol), and dichloromethane (50 mL) were placed in a Schlenk tube and stirred at room temperature for 48 h. During the course of the reaction the dark mixture slowly changed to orange. The solvent was removed in vacuo and the residue washed with hexane (3 \times 20 mL) and cold CH₂Cl₂ (2 \times 10 mL) to give **3a** as an orange paramagnetic solid. Yield: 1.80 g (85%). Anal. Calc for C₁₅H₁₈N₂OSiBr₂Ni (488.91): C, 36.85; H, 3.71; N, 5.73; O, 3.27. Found: C, 37.14; H, 3.92; N, 5.79; O, 3.13. IR (Nujol/CsI): ν 1624 cm⁻¹ (w), 1596 cm⁻¹ (vs, C=N), 1559 cm⁻¹ (w). MS (70 eV, EI): *m/z* 409 [M – Br]⁺, 270 [2a]⁺; (ESI+ in CH₃CN) *m/z* 450 [M – Br + CH₃CN]⁺.

NiBr₂[Me₃SiO-4-(2,5-Me₂Ph)-N=CH-2-(6-MePy)] (3c): red, paramagnetic solid. Yield: 68%. Anal. Calc for C₁₈H₂₄N₂OSiBr₂Ni (530.99): C, 40.72; H, 4.56; N, 5.28. Found: C, 40.70; H, 4.17;

Table 4. Crystal Data and Structure Refinement for Compounds **3c** and **4**

	3c·H ₂ O	4·(H ₂ O) ₂
empirical formula	C ₁₈ H ₂₆ Br ₂ N ₂ NiO ₂ Si	C ₂₄ H ₂₄ Br ₂ N ₄ NiO ₄
fw	549.03	650.98
color	red	red
temperature	200(2) K	100(2) K
wavelength	0.71073 Å	0.71073 Å
cryst syst, space group	monoclinic, <i>P2₁</i>	orthorhombic, <i>Pbcn</i>
unit cell dimens	<i>a</i> = 14.797(7) Å <i>b</i> = 7.446(4) Å; β = 107.87(3) ^o <i>c</i> = 21.455(11) Å	<i>a</i> = 15.3360(3) Å <i>b</i> = 9.4940(8) Å <i>c</i> = 16.9100(8) Å
volume	2250(2) Å ³	2462.1(2) Å ³
Z, calcd density	4, 1.621 g/cm ³	4, 1.756 g/cm ³
absorp coeff	44.8 cm ⁻¹	40.73 cm ⁻¹
<i>F</i> (000)	1104	1304
cryst size	0.35 × 0.27 × 0.2 mm	0.4 × 0.35 × 0.3 mm
θ ranges	5.00 to 27.53 ^o	2.41 to 27.50 ^o
limiting indices	-15 ≤ <i>h</i> ≤ 19, -9 ≤ <i>k</i> ≤ 8, -27 ≤ <i>l</i> ≤ 25	-19 ≤ <i>h</i> ≤ 19, -12 ≤ <i>k</i> ≤ 12, -18 ≤ <i>l</i> ≤ 21
no. of reflns collected/unique	11527/4876 [<i>R</i> (int) = 0.11781]	48364/2829 [<i>R</i> (int) = 0.0381]
no. of reflns obsd	2767	2502 [<i>I</i> > 2 σ (<i>I</i>)]
absorp corr	multiscan	none
max. and min. transmn	1.476, 0.079	
refinement method	full-matrix least-squares on <i>F</i> ²	full-matrix least-squares on <i>F</i> ²
no. of data/restraints/params	4876/0/263	2829/0/167
goodness of fit on <i>F</i> ²	1.014	0.933
final <i>R</i> ^a indices [<i>I</i> > 2 σ (<i>I</i>)]	<i>R</i> ₁ = 0.0727, <i>wR</i> ₂ = 0.1341	<i>R</i> ₁ = 0.021, <i>wR</i> ₂ = 0.0506
<i>R</i> indices (all data)	<i>R</i> ₁ = 0.1476, <i>wR</i> ₂ = 0.1616	<i>R</i> ₁ = 0.0259, <i>wR</i> ₂ = 0.053
largest diff peak and hole	1.017 and -1.205 e/Å ³	0.477 and -0.638 e/Å ³

$$^a R_1 = \sum ||F_o| - |F_c|| / \sum |F_o|; wR_2 = \{[\sum w(F_o^2 - F_c^2)] / [\sum w(F_o^2)]\}^{1/2}.$$

N, 5.14. IR (KBr): ν 1627 cm⁻¹ (w), 1595 cm⁻¹ (vs, C=N), 1565 cm⁻¹ (w). MS (70 eV, EI): *m/z* 531 [M]⁺, 451 [M - Br]⁺, 371 [M - 2Br]⁺, 312 [2c]⁺; (ESI+ and APCI in CH₃CN) *m/z* 492 [M - Br + CH₃CN]⁺, 313 [2c + H]⁺.

NiBr₂(HO-4-Ph-N=CH-2-Py)₂ (4). Ethanol (30 mL) was added to a mixture of ligand **1a** (0.77 g, 3.9 mmol) and [NiBr₂(DME)] (0.60 g, 1.94 mmol). The dark red solution was stirred overnight at room temperature and then added dropwise over pentane (150 mL) and vigorously stirred. The precipitated solid was separated by filtration and dried under vacuum to give **4** analytically pure, as a red, paramagnetic solid. Yield: 1.12 g (94%). Crystalline **4** was also obtained in attempts to recrystallize **3a** from ethanol/pentane as a solvent mixture. Anal. Calc for C₂₄H₂₀N₄O₂Br₂Ni (614.95): C, 46.88; H, 3.28; N, 9.11. Found: C, 47.11; H, 3.42; N, 8.99. IR (Nujol/CsI): ν 1623 cm⁻¹ (m), 1592 cm⁻¹ (vs, C=N), 1563 cm⁻¹ (m). MS (70 eV, EI): *m/z* 197 [1a - H]⁺; (ESI+ in CH₃CN) *m/z* 535 [M - Br]⁺, 198 [1a]⁺.

X-ray Crystallographic Studies. Suitable monocrystals of **3c** were obtained from a dichloromethane solution exposed to air, and by slow diffusion of a pentane layer into an ethanol solution in the case of complex **4**. A summary of crystal data, data collection, and refinement parameters for the structural analysis is given in Table 4. Red crystals of the compounds **3c** or **4** were glued to a glass fiber using an inert polyfluorinated oil and mounted in an N₂ stream in a Bruker-Nonius Kappa-CCD diffractometer with area detector, and data were collected using graphite-monochromated Mo K α radiation (λ = 0.71073 Å). Data for compound **3c** were collected at low temperature (200 K), with an exposure time of 34 s per frame (four sets; 263 frames; omega scans 1.7^o scan-width). Data for compound **4** were collected at low temperature (100 K), with an exposure time of 30 s per frame (six sets; 939 frames; phi and omega scans 1.0^o scan-width). Raw data were corrected for Lorentz and polarization effects.

Structures were solved by direct methods, completed by substructure difference Fourier techniques, and refined by full-matrix least squares on *F*² (SHELXL-97).⁵² Anisotropic thermal parameters were used in the last cycles of refinement for the non-hydrogen atoms

in both structures. Hydrogen atoms were included from geometrical calculations and refined using a riding model. All the calculations were made using the WINGX system.⁵³

Preparation of G1-Pyridylimine Dendritic Ligands (5). Terminal-functionalized carbosilanes **5a-c** were prepared as illustrated for **5a**. Characterization data for **5b** have already been reported in a previous account.^{33d}

G1-ONN (5a). A solution of chlorosilane G1-Cl (2.45 g, 4.3 mmol) in THF (20 mL) was added via cannula to a stirred mixture of **1a** (3.45 g, 17.4 mmol) and Et₃N (2.5 mL, 18 mmol) in THF (40 mL) at 0 °C. The reaction was allowed to proceed at room temperature overnight, precipitating Et₃N·HCl. The white solid was separated by filtration, the solvent of the filtrate was removed at reduced pressure, and the yellow residue was extracted with diethyl ether or toluene (2 × 30 mL). The yellow viscous oil obtained after solvent evaporation was characterized as **5a**, which was found to be soluble in all common organic solvents. Yield: 5.20 g (99%). Anal. Calc for C₆₈H₈₄N₈O₄Si₅ (1217.89): C, 67.06; H, 6.95; N, 9.20. Found: C, 66.40; H, 7.09; N, 9.36. ¹H NMR (CDCl₃): δ 0.22 (s, 6H, SiMe₂), 0.58 (m, 2H, SiCH₂), 0.80 (m, 2H, CH₂SiMe₂), 1.41 (m, 2H, CH₂CH₂CH₂), 6.84 (AA' part of an AA'BB' spin system, 2H, H^{3,5}), 7.22 (BB' part of an AA'BB' spin system, 2H, H^{2,6}), 7.31 (m, 1H, H¹¹), 7.75 (m, 1H, H¹⁰), 8.14 (d, 1H, *J*_{H,H} = 8.0 Hz, H⁹), 8.58 (s, 1H, H⁷), 8.66 (d, 1H, *J*_{H,H} = 4.8 Hz, H¹²). ¹³C-{¹H} NMR (CDCl₃): δ -1.2 (SiMe₂), 17.0 (CH₂), 17.7 (CH₂), 21.4 (CH₂), 120.5 (C^{3,5}), 121.6 (C⁹), 122.6 (C^{2,6}), 124.8 (C¹¹), 136.6 (C¹⁰), 144.2 (C¹), 149.5 (C¹²), 154.7 (C⁴), 154.8 (C⁸), 158.2 (C⁷). ²⁹Si{¹H} NMR (CDCl₃): δ 19.5 (SiMe₂), 0.7 (central Si). IR (Nujol/CsI): ν 1626 cm⁻¹ (s, C=N), 1596 (w, C=C), 1582 and 1568 cm⁻¹ (vs and s, py-ring).

G1-ONNMe₃ (5c): yellow, viscous oil. Yield: 97%. Anal. Calc for C₈₀H₁₀₈N₈O₄Si₅ (1386.22): C, 69.32; H, 7.85; N, 8.08. Found: C, 69.32; H, 8.25; N, 8.04. ¹H NMR (CDCl₃): δ 0.21 (s, 6H, SiMe₂), 0.59 (m, 2H, SiCH₂), 0.80 (m, 2H, CH₂SiMe₂), 1.42 (m, 2H, CH₂CH₂CH₂), 2.12 (s, 3H, Me¹⁴), 2.32 (s, 3H, Me¹³), 2.59 (s, 3H, Me¹⁵), 6.60 (s, 1H, H³), 6.91 (s, 1H, H⁶), 7.16 (d, 1H, *J*_{H,H} = 7.5 Hz, H¹¹), 7.63 (pt, 1H, H¹⁰), 8.01 (d, 1H, *J*_{H,H} = 7.5 Hz, H⁹), 8.48 (s, 1H, H⁷). ¹³C-{¹H} NMR (CDCl₃): δ -0.9 (SiMe₂), 16.4 and

(52) Sheldrick, G. M. *SHELXL-97. Program for Crystal Structure Refinement* (Release 97-2); University of Göttingen: Göttingen, Germany, 1998.

(53) WinGX System. Farrugia, L. J. *J. Appl. Crystallogr.* **1999**, *32*, 837.

17.7 (Me^{13,14}), 17.1 (CH₂), 17.9 (CH₃), 21.9 (CH₂), 24.4 (Me¹⁵), 118.3 (C³), 119.6 (C⁶), 120.5 (C⁹), 124.1 (C¹¹), 126.7 (C⁵), 131.7 (C²), 136.6 (C¹⁰), 142.8 (C¹), 152.5 (C⁴), 154.7 (C⁸), 157.6 (C⁷), 158.0 (C¹²). ²⁹Si{¹H} NMR (CDCl₃): δ 18.2 (SiMe₂), 0.7 (central Si). IR (Nujol/CsI): ν 1626 cm⁻¹ (s, C=N), 1589 and 1573 cm⁻¹ (vs and s, py-ring). MS (ESI+ in CH₃CN): *m/z* 1087 [M - 1c - SiMe₂]⁺. MS (MALDI-TOF in dithranol): *m/z* 1386.7 [M + H]⁺.

Preparation of G2-Pyridylimine Dendritic Ligands (6). Carbosilane dendrimers **6a–c** were prepared as illustrated for **6a**, starting from the corresponding hydroxyphenylpyridylimines **1**. Characterization data for **6b** have already been reported in a previous communication.^{33d} Dendrimers **6b,c** were purified by silica gel chromatography using CH₂Cl₂ (**6b**) or ethyl acetate (**6c**) as eluents.

G2-ONN (6a). A solution of chlorosilane dendrimer G2-Cl (2.11 g, 1.45 mmol) in THF (15 mL) was added to a mixture of **1a** (2.31 g, 11.6 mmol) and Et₃N (2.0 mL, 14 mmol) in THF (30 mL) at 0 °C. The white suspension was stirred overnight at room temperature. Then, the solvent was removed at reduced pressure, and the residue extracted with toluene (3 × 30 mL). Removal of the toluene afforded **6a** as a brownish, sticky oil. Yield: 3.00 g (75%). Anal. Calc for C₁₅₂H₂₀₄N₁₆O₈Si₁₃ (2748.51): C, 66.42; H, 7.48; N, 8.15. Found: C, 66.14; H, 7.41; N, 8.34. ¹H NMR (CDCl₃): δ -0.08 (s, 3H, SiMe), 0.22 (s, 12H, SiMe₂), 0.57 (m, 8H, SiCH₂), 0.80 (m, 4H, CH₂SiMe₂), 1.29 (m, 2H, CH₂CH₂CH₂), 1.41 (m, 4H, CH₂CH₂CH₂), 6.83 (AA' part of an AA'BB' spin system, 4H, H^{3,5}), 7.21 (BB' part of an AA'BB' spin system, 4H, H^{2,6}), 7.30 (m, 2H, H¹¹), 7.75 (m, 2H, H¹⁰), 8.14 (d, 2H, J_{H,H} = 7.6 Hz, H⁹), 8.58 (s, 2H, H⁷), 8.66 (d, 2H, J_{H,H} = 4.0 Hz, H¹²). ¹³C{¹H} NMR (CDCl₃): δ -5.0 (SiMe), -1.1 (SiMe₂), 17.7, 18.4, 18.6, 19.1, 21.4, and 21.5 (CH₂), 120.5 (C^{3,5}), 121.5 (C⁹), 122.5 (C^{2,6}), 124.7 (C¹¹), 136.4 (C¹⁰), 144.1 (C¹), 149.4 (C¹²), 154.5 (C⁴), 154.6 (C⁸), 158.1 (C⁷). IR (Nujol/CsI): ν 1627 cm⁻¹ (s, C=N), 1596 (w, C=C), 1582 and 1568 cm⁻¹ (vs and s, py-ring).

G2-ONNMe₃ (6c): brownish, viscous oil. Yield: 57%. Anal. Calc for C₁₇₆H₂₅₂N₁₆O₈Si₁₃ (3085.15): C, 68.52; H, 8.23; N, 7.26. Found: C, 68.42; H, 8.70; N, 7.14. ¹H NMR (CDCl₃): δ -0.08 (s, 3H, SiMe), 0.20 (s, 12H, SiMe₂), 0.57 (m, 8H, SiCH₂), 0.80 (m, 4H, CH₂SiMe₂), 1.29 (m, 2H, CH₂CH₂CH₂), 1.42 (m, 4H, CH₂CH₂CH₂), 2.12 (s, 6H, Me¹⁴), 2.32 (s, 6H, Me¹³), 2.58 (s, 6H, Me¹⁵), 6.60 (s, 2H, H³), 6.90 (s, 2H, H⁶), 7.15 (d, 2H, J_{H,H} = 7.7, H¹¹), 7.62 (pt, 2H, H¹⁰), 8.00 (d, 2H, J_{H,H} = 7.2 Hz, H⁹), 8.47 (s, 2H, H⁷). ¹³C{¹H} NMR (CDCl₃): δ -5.0 (SiMe), -0.9 (SiMe₂), 16.3 and 17.6 (Me^{13,14}), 17.8, 18.5, 18.6, 19.2, and 21.8 (CH₂), 24.3 (Me¹⁵), 118.4 (C³), 119.7 (C⁶), 120.7 (C⁹), 124.2 (C¹¹), 126.8 (C⁵), 131.7 (C²), 136.6 (C¹⁰), 143.0 (C¹), 152.7 (C⁴), 154.9 (C⁸), 157.8 (C⁷), 158.1 (C¹²). ²⁹Si{¹H} NMR (CDCl₃): δ 18.0 (SiMe₂), 0.8 (SiMe), 0.1 (central Si). IR (Nujol/CsI): ν 1626 cm⁻¹ (s, C=N), 1589 and 1572 cm⁻¹ (vs and s, py-ring). MS (MALDI-TOF in dithranol): *m/z* 3085.8 [M + H]⁺.

Preparation of G3-Pyridylimine Dendritic Ligands (7). Carbosilane dendrimers **7b,c** were prepared as illustrated for **7c**. The data for **7b** have been reported previously.^{33d} **7b** was purified by silica gel chromatography using CH₂Cl₂ as eluent.

G3-ONNMe₃ (7c). A solution of chlorosilane dendrimer G3-Cl (0.87 g, 0.27 mmol) in THF (15 mL) was added to a mixture of **1c** (1.05 g, 4.39 mmol) and Et₃N (1.0 mL, 7.2 mmol) in THF (40 mL) at 0 °C. The white suspension was stirred overnight at room temperature, the solvent was then removed at reduced pressure, and the residue was extracted with toluene (3 × 30 mL) and further purified by silica gel chromatography in ethyl acetate. Dendrimer **7c** was isolated as a brownish oil, soluble in all common organic solvents. Yield: 1.68 g (96%). Anal. Calc for C₃₆₈H₅₄₀N₃₂O₁₆Si₂₉ (6483.02): C, 68.18; H, 8.40; N, 6.91. Found: C, 68.35; H, 8.90; N, 6.39. ¹H NMR (CDCl₃): δ -0.09 (s, 9H, SiMe), 0.20 (s, 24H, SiMe₂), 0.55 (m, 20H, SiCH₂), 0.79 (m, 8H, CH₂SiMe₂), 1.28 (m, 6H, CH₂CH₂CH₂), 1.41 (m, 8H, CH₂CH₂CH₂), 2.11 (s, 12H, Me¹⁴),

2.31 (s, 12H, Me¹³), 2.58 (s, 12H, Me¹⁵), 6.59 (s, 4H, H³), 6.89 (s, 4H, H⁶), 7.13 (d, 4H, J_{H,H} = 7.0, H¹¹), 7.60 (pt, 4H, H¹⁰), 7.99 (d, 4H, J_{H,H} = 7.2 Hz, H⁹), 8.46 (s, 4H, H⁷). ¹³C{¹H} NMR (CDCl₃): δ -4.7 (SiMe), only one peak can be distinguished), -0.7 (SiMe₂), 16.6 and 17.8 (Me^{13,14}), 18.0, 18.7, 19.2, and 21.9 (CH₂), 24.5 (Me¹⁵), 118.1 (C³), 119.5 (C⁶), 120.4 (C⁹), 124.0 (C¹¹), 126.6 (C⁵), 131.5 (C²), 136.4 (C¹⁰), 142.6 (C¹), 152.3 (C⁴), 154.4 (C⁸), 157.3 (C⁷), 157.6 (C¹²). ²⁹Si{¹H} NMR (CDCl₃): δ 17.9 (SiMe₂), 0.7 (outermost SiMe), 0.5 (SiMe), 0.0 (central Si). IR (Nujol/CsI): ν 1626 cm⁻¹ (s, C=N), 1589 and 1572 cm⁻¹ (s, py-ring).

Preparation of G1-Pyridylimine-NiBr₂ Dendritic Complexes (8). Compounds **8a–c** were synthesized as described above for **3** starting from the corresponding G1-pyridylimine dendritic ligands (**5**). The preparation of **8a** is reported as an example, whereas characterization data for **8b** have been reported previously.^{33d}

G1-ONNNiBr₂ (8a). [NiBr₂(DME)] (697 mg, 2.26 mmol) was added to a solution of compound **G1-ONN (5a)** (688 mg, 0.56 mmol) in dichloromethane (25 mL), and the mixture was stirred at room temperature for 3 days. A yellow solid precipitated out of the dark suspension, which was separated by filtration and washed with CH₂Cl₂ (3 × 20 mL) and hexane (3 × 20 mL) to give **8a** as a yellow paramagnetic solid scarcely soluble in any common solvents. Yield: 804 mg (69%). Anal. Calc for C₆₈H₈₄N₈O₄Si₅Br₂Ni₄: C, 39.04; H, 4.05; N, 5.36. Found: C, 39.10; H, 4.20; N, 5.12. IR (Nujol/CsI): ν 1622 cm⁻¹ (w), 1597 cm⁻¹ (vs, C=N), 1560 cm⁻¹ (w).

G1-ONNMe₃NiBr₂ (8c): orange, paramagnetic solid soluble in CH₂Cl₂. Yield: 60%. Anal. Calc for C₈₀H₁₀₈N₈O₄Si₅Br₂Ni₄ (2260.22): C, 42.51; H, 4.82; N, 4.96. Found: C, 42.96; H, 5.11; N, 4.88. IR (Nujol/CsI): ν 1625 cm⁻¹ (w), 1595 cm⁻¹ (vs, C=N), 1561 cm⁻¹ (w). MS (MALDI-TOF in dithranol): *m/z* 2180.3 [M - Br]⁺.

Preparation of G2- and G3-Pyridylimine-NiBr₂ Dendritic Complexes (9 and 10b). Compounds **9a,b** and **10b** were synthesized similarly to that described above for **3** starting from the corresponding *Gn*-pyridylimine dendritic ligands (**6** or **7b**). The preparation of **9a** is reported as an example, and data for compounds **9b** and **10b** have been reported previously.^{33d}

G2-ONNNiBr₂ (9a). [NiBr₂(DME)] (152 mg, 0.49 mmol) suspended in dichloromethane (50 mL) was added to a solution of compound **G2-ONN (6a)** (170 mg, 0.06 mmol) in the same solvent (25 mL), and the mixture was stirred at room temperature for 3 days. A yellow solid precipitated out of the dark mixture, which was separated by filtration and washed with CH₂Cl₂ (3 × 15 mL) and hexane (3 × 20 mL) to give **9a** as a yellow, paramagnetic solid scarcely soluble in any common solvents. Yield: 220 mg (81%). Anal. Calc for C₁₅₂H₂₀₄N₁₆O₈Si₁₃Ni₈Br₁₆ (4496.52): C, 40.60; H, 4.57; N, 4.98. Found: C, 40.18; H, 5.30; N, 5.04. IR (KBr): ν 1625 cm⁻¹ (m), 1599 cm⁻¹ (vs, C=N), 1560 cm⁻¹ (w).

General Procedure for Ethylene Catalytic Reactions. Ethylene was prepurified by passage through an ALLTECH gas purification system (AT-Indicating Oxy Cartridge). The corresponding catalyst precursor was weighed (5–10 mg) into a 250 mL screw-capped glass pressure reactor equipped with a mechanical stirrer. The reactor was capped and sealed with a septum, purged by repeated argon/vacuum operations, charged with purified toluene (50 mL), and flushed with ethylene gas fed at constant pressure (2 bar). Polymerization was initiated, at least, 10 min later by the addition of a toluene solution of PMAO-IP (Al/Ni = 1000) with vigorous stirring. After a desired time interval the ethylene pressure was released, the polymerization reaction was quenched with acidified methanol (2% HCl), and the mixture was stirred overnight. The polymer was filtered, washed with methanol, and dried in an oven to constant weight. The reaction filtrate was washed with water and treated with MgSO₄, and the volatiles were removed in a rotary evaporator. To minimize experimental error, the polymerization data represent the average of a number of runs disregarding the data

from those with yields deviating more than 7%. The mixtures of oligomers were analyzed by GC in pentane as a solvent. The Schulz–Flory α parameter of each sample ($\alpha = \text{mol of } C_{n+2}/\text{mol of } C_n$) was calculated as described below from the GC data and the equation $\log(\text{mol } \% \text{ of } C_n) = 2n \log \alpha + A$, where n is the chain length in carbon number and A is a constant (see for instance Supporting Information in ref 41c). First, the data of lighter olefins (below C_{16}) were omitted because they are partially or completely lost by evaporation in the workup procedure, and only the heavier oligomers that gave well-resolved peaks of significant area in the GC of the considered sample were utilized for calculations (minimum from C_{16} up to C_{24} and usually up to C_{30} , between 5 and 8 data points). Subsequently, the product distribution of the selected oligomers, expressed as $\log(\text{mol } \% \text{ of oligomer})$, was plotted versus the oligomer chain length n . As expected for a Schulz–Flory distribution, least-squares linear fits of reasonably good quality (correlation coefficients in the range 0.960–0.999) were obtained for all the samples. Finally, the α parameter

determined from the linear fitting was used to estimate the quantity of lower olefins lost in the workup.⁸ The microstructure of these materials was also determined by ^1H NMR (oligomers, rt, CDCl_3) or $^{13}\text{C}\{^1\text{H}\}$ NMR (polymers, 100 °C, 20% v/v benzene- d_6 /TCB).

Acknowledgment. We acknowledge the financial support from the DGI-Ministerio de Educación y Ciencia (project CTQ2005-00795/BQU) and Comunidad de Madrid (project GR/MAT/0733/2004). In addition, we thank Dr. Carmen Martínez and Dr. Carlos Martín, REPSOL YPF, for their valuable assistance with ^{13}C NMR polymer analyses.

Supporting Information Available: The CIF files for compounds **3c**· H_2O and **4** are available free of charge at <http://pubs.acs.org>.

OM0509084